Biochemical and conformational characterisation of HSP-3, a stallion seminal plasma protein of the cysteine-rich secretory protein (CRISP) family

Leticia Magdaleno[a], María Gasset[a], Julio Varea[a], Alexandra M. Schambony[b], Claus Urbanke[c], Manfred Raida[d], Edda Töpfer-Petersen[1,b], Juan J. Calvete[a,b]

[a]*Instituto de Química-Física 'Rocasolano', C.S.I.C., Madrid, Spain*
[b]*Institut für Reproduktionsmedizin, Tierärztliche Hochschule, Bünteweg 15, D-30559 Hannover-Kirchrode, Germany*
[c]*Medizinische Hochschule, Meßgeräteabteilung, Hannover, Germany*
[d]*Niedersächsisches Institut für Peptid-Forschung (IPF) GmbH, Hannover, Germany*

Received 14 November 1997

Abstract HSP-3 is a member of the cysteine-rich secretory protein (CRISP) family from stallion seminal plasma. We report a large-scale purification protocol for native HSP-3. This protein is a non-glycosylated polypeptide chain with a p*I* of 8–9 and an isotope-averaged molecular mass of 24 987 ± 3 Da. The molecular mass of HSP-3, determined by equilibrium sedimentation, is 26 kDa, showing that the protein exists in solution as a monomer. The concentration of HSP-3 in the seminal plasma of different stallions ranged from 0.3 to 1.3 mg/ml. On average, 0.9–9 million HSP-3 molecules/cell coat the postacrosomal and mid-piece regions of an ejaculated, washed stallion spermatozoon, suggesting a role in sperm physiology. Conformational characterisation of purified HSP-3 was assessed by combination of circular dichroism and Fourier-transform infrared spectroscopies and differential scanning microcalorimetry. Based on secondary structure assignment, HSP-3 may belong to the α+β class of proteins. Thermal denaturation of HSP-3 is irreversible and follows a non-two state transition characterised by a T_m of 64°C, an enthalpy change of 75 kcal/mol, and a van 't Hoff enthalpy of 184 kcal/mol. Analysis of the spectroscopic and calorimetric data indicates the occurrence of aggregation of denatured HSP-3 molecules and suggests the monomer as the cooperative unfolding unit.

Key words: Horse seminal plasma protein; HSP-3; Cysteine-rich secretory protein; Mass spectrometry; Conformational analysis

1. Introduction

Mammalian fertilisation involves a sequence of specific and well orchestrated interactions between homologous gametes (reviewed in [1]). After getting round the cumulus cell mass surrounding the egg at ovulation, capacitated spermatozoa bind to glycoconjugates of the oocyte's extracellular coat, the zona pellucida. This glycoprotein matrix induces the acrosome reaction, an exocytotic event by which proteolytic enzymes (e.g. acrosin) are liberated aiding acrosome-reacted spermatozoa to penetrate the zona pellucida. In eutherian mammals, the fusion of the plasma membranes of the oocyte (oolemma) and the equatorial segment and posterior head regions of a spermatozoon that crosses the perivitelline space [2–4] is the last cellular interaction of mammalian fertilisation, and the event that gives the signal to begin development. Each of these steps requires interactions between sets of complementary molecules expressed on specific regions of the gamete surface.

The molecular mechanisms underlying sperm-egg membrane binding and fusion in mammals are poorly understood. Sperm-egg fusion is temperature- and pH-dependent, and requires millimolar concentrations of extracellular Ca^{2+} [1]. Factors implicated in the development of the sperm's fusion capability include spermatozoal adhesion molecules which migrate to, or are unmasked on, the equatorial segment/posterior head region concomitantly with the occurrence of the acrosome reaction. Recently, antibody inhibition studies have allowed the identification of surface molecules of gametes of several mammalian species involved in these processes (reviewed in [5–9]).

A mammalian sperm fusion candidate is protein DE [10,11], a 227-residue androgen-dependent sperm-coating glycoprotein secreted by the proximal segments of the rat epididymis [12]. Protein DE, originally localised on the dorsal region of the sperm head, migrates to the equatorial segment concomitantly with the occurrence of the acrosome reaction [13] and is believed to participate in sperm-egg fusion by binding to complementary sites on the egg plasma membrane [8,14]. Recently, it has been shown that protein DE belongs to an emerging superfamily of secretory proteins collectively termed CRISP (for cysteine-rich secretory proteins) [15]. Human, murine, rat, guinea, pig, and lizard CRISP family members display 40–80% amino acid sequence identity [15–17]. CRISP-1 transcripts are epididymis-specific, whereas CRISP-2 transcripts are secreted mainly in the testis but also in the epididymis. CRISP-3 transcripts are widely distributed and found predominantly in salivary gland, pancreas, and prostate [15]. In stallion seminal plasma we have identified a 27 kDa protein (called horse seminal plasma protein 3, or HSP-3), which displays extensive amino acid sequence similarity with CRISPs [18]. Here we report the biochemical and conformational characterisation of HSP-3.

2. Methods

2.1. Isolation and biochemical characterisation of HSP-3

For HSP-3 isolation, 100–500 ml of stallion seminal plasma (a generous gift of Dr. Harald Sieme, Celle, Germany) was applied to a 2.6×18 cm heparin-Sepharose (Pharmacia) column equilibrated in 10 mM Tris-HCl, 150 mM NaCl, 5 mM EDTA, 0.025% sodium azide,

[1]Corresponding author. Fax: (49) (511) 953 8504.
E-mail: JCalvete@Repro.TiHo-Hannover.De or ETP@Repro.TiHo-Hannover.De

0014-5793/97/$17.00
PII S0014-5793(97)01514-7

pH 7.4 (TBS buffer). The non-heparin-binding fraction was concentrated to 50 ml by ultrafiltration (using a PM10 Amicon membrane) and chromatographed on a 0.8×15 cm *p*-aminophenyl phosphorylcholine (PC)-agarose (Pierce) column equilibrated in TBS. Proteins HSP-1 and HSP-2 [18], which are the major contaminants of HSP-3-enriched gel-filtration fractions, possess affinity for phosphorylcholine [19] and are retained in the column. HSP-3, recovered in the non-PC-binding fraction, was concentrated to about 50 ml and was chromatographed on two 5×90 cm Sephadex G50 (Pharmacia) columns connected in series and equilibrated in TBS. Samples along the size-exclusion chromatographic profile were subjected to SDS-polyacrylamide gel electrophoresis. Gels were visualised by staining with Coomassie blue or electrotransferred to a nitrocellulose membrane and probed with a polyclonal monospecific anti-HSP-3 antibody (using a standard immunoblotting procedure). This antibody was raised in chicken by immunisation against pure HSP-3 isolated by reverse-phase HPLC [18]. If necessary, HSP-3 was finally purified by rechromatography on the Sephadex-G50 columns as above. The purity of HSP-3 was assessed by reversed-phase HPLC [18], electrospray ionisation mass spectrometry (using a Sciex API-III MS/Ms/MS triple quadrupole instrument), and by two-dimensional electrophoresis [20] using 11 cm long Immobiline Dry-Strips (pH 3–10) (Pharmacia) for isoelectric focusing (20 h at 15°C and 22.650 Vh). Sample buffer was 9 M urea, 2% (v/v) Nonidet P40. The second dimension was performed using SDS-(15%) polyacrylamide gels. Gels were silver-stained according to [21].

Amino acid analysis, carbohydrate analyses and quantitation of free cysteine residues and disulphide bonds were done as described [19].

Quantitation of HSP-3 in stallion seminal plasma, ejaculated sperm and washed spermatozoa (three times in PBS, pH 7.4, by centrifugation at 100×*g* for 10 min at room temperature), and chromatographic fractions obtained during the HSP-3 purification protocol was determined by competitive ELISA as described [22].

Before use, protein samples for conformational studies were extensively dialysed at 4°C against 20 mM HEPES pH 7.0. Protein concentration was determined spectrophotometrically using an extinction coefficient ($E_{280,1mg/ml}$) of 2.5, determined by amino acid analysis of aqueous HSP-3 solutions of defined absorbance at 280 nm measured in 1 cm pathlength quartz cuvettes.

2.2. Immunolocalisation of HSP-3 on stallion spermatozoa

Localisation of HSP-3 epitopes on ejaculated stallion spermatozoa was studied by indirect immunofluorescence. Spermatozoa were separated from seminal plasma, and washed three times with 20 mM sodium phosphate, 135 mM NaCl, pH 7.4 (PBS buffer), by centrifugation (500×*g*, 10 min, 20°C). 10 μl of the sperm suspension was spread on slides, air-dried, and fixed for 15 min in methanol. The preparations were incubated overnight at 4°C with PBS containing 50 mg/ml BSA (blocking buffer), followed by incubation with either blocking buffer (control) or 100 μl of a 1:3000 chicken anti-HSP-3 antibody solution for 2 h at 37°C in a humid chamber. After washing three times for 10 min each with PBS containing 0.5% BSA (washing buffer), both samples were incubated for 1 h at 37°C with 100 μl of biotinylated anti-chicken IgG (diluted 1:500 in washing buffer), washed three times, and incubated for 1 h at 37°C with 100 μl 5 μg/ml streptavidin-FITC. The preparations were exhaustively washed with washing buffer, and observed under a fluorescence microscope (Zeiss, 100×10 magnification). Controls were run by omission of the primary antibody and by replacement of the primary antibody with preimmune serum.

2.2.1. Sedimentation velocity. Sedimentation velocity runs of HSP-3 (0.3–1.5 mg/ml in PBS, pH 7.4) were performed in a Beckman XL-A analytical ultracentrifuge with absorption optics at 60 000 rpm and 20°C using standard double sector cells. For equilibrium sedimentation measurements six-channel cells were used allowing the simultaneous analysis of nine samples containing initially 0.3 mg/ml HSP-3 in PBS, pH 7.4 and different concentrations of guanidinium hydrochloride. Equilibrium sedimentation runs were performed at 18 000 and 30 000 rpm and 20°C. Based on the amino acid composition of HSP-3, a partial specific volume of 0.726 ml/g was considered.

2.2.2. Circular dichroism. Circular dichroism (CD) spectra were recorded in a JASCO J-720 spectropolarimeter fitted with a thermostatted cell holder and interfaced to a thermostatic bath, as previously described [23]. Far-UV spectra were recorded in 0.1 cm pathlength quartz cells at a protein concentration of about 0.15 mg/ml. Near-UV spectra were collected in 1 cm pathlength quartz cuvettes using a protein concentration of 1 mg/ml. The observed ellipticities were converted to mean residue ellipticities [θ] on the basis of a mean molecular mass per residue of 110 Da. Thermal denaturation experiments were carried out by increasing the temperature from 20 to 90°C at 0.5°C/min, allowing temperature equilibration for 5 min. Far-UV spectrum deconvolution was performed by the Limbcom method [24] using the chiroptic components derived by convex constraint analysis (CCA) [25] from the original protein reference data set (which includes 25 proteins) and the experimental data of the following β-sheet-rich proteins that display strong non-peptide chirality: barnase [26], fibroblast acidic growth factor [27], and PSPI-PSPII [23].

2.2.3. Infrared spectra. Infrared spectra were recorded in a Perkin-Elmer 1725X Fourier-transform infrared (FTIR) spectrometer equipped with a HgCdTe detector and continuously purged with dried air. For each spectrum a total of 200 scans at 2 cm^{-1} resolution were co-added. Protein aliquots of 300 μg were dried under N_2 flow and hydrated by adding 30 μl of 20 mM MOPS buffer pH 7.0 prepared in D_2O. Samples were left for 4 h at 10°C to allow isotopic substitution of protein exchangeable NH groups, and were then placed between two CaF_2 discs separated by a 25 μm Teflon spacer and mounted on a thermostatically controlled cell holder. Longer exposures to the solvent did not produce further spectral changes. Thermal denaturation experiments were performed raising the temperature in 3–4°C steps, allowing 10 min for equilibration before spectrum acquisition. Temperature was measured in situ with a thermocouple probe. Overlapping bands were resolved by Fourier self-deconvolution with a Lorentzian line shape (full width at half-height = 30 cm^{-1}), a Gaussian line shape for apodisation and a resolution enhancement factor (*k*) of 1.8 [28]. Secondary structure analysis was performed by least-square iterative curve fitting of the non-deconvoluted amide I′ band to Lorentzian curves as previously described [28]. The assignment of the Lorentzian components to the different secondary structures was carried out according to the frequency maximum as follows: 1682–1662.5 cm^{-1}, turns; 1662.5–1647 cm^{-1}, α-helix and solvent-shielded loops; 1647–1637 cm^{-1}, non-ordered and solvent-exposed loops; 1637–1627 cm^{-1}, β-sheet; and 1627–1615 cm^{-1}, low-frequency (LF) β-sheet. The amide II/amide I′ area ratios were determined from the integrals of the amide II [$(1600 \pm 6)-(1500 \pm 12)$, cm^{-1}] and amide I′ [$(1700 \pm 4)-(1600 \pm 6)$, cm^{-1}] bands.

2.2.4. Calorimetric measurements. Calorimetric measurements were performed in a Microcal MCS differential scanning microcalorimeter (Microcal Inc., Northampton, MA) at a heating rate of 0.33 K/min, unless otherwise stated, and under an extra constant pressure of 2 atm (200 kPa). The Microcal Origin software was used for data acquisition and analysis. The excess heat capacity functions were obtained after buffer-buffer baseline subtraction. HSP-3 samples were prepared at about 1.0 mg/ml protein concentration. Reversibility of thermal denaturation was studied by reheating the samples after the first scan. The influence of scanning conditions on calorimetric irreversible profiles was checked running the samples at several heating rates.

3. Results and discussion

3.1. Isolation and molecular characterisation of HSP-3

HSP-3 is an abundant component of stallion seminal plasma [18] and a novel member of the androgen-dependent CRISP family originally described in the mouse reproductive tract, and more recently found predominantly in the salivary glands of several species [15]. Quantitation of HSP-3 in the seminal plasma of different stallions by competitive ELISA showed a large variation of its concentration, ranging from 0.3 to 1.3 mg/ml. On the other hand, we have failed in identifying CRISP homologous molecules in the seminal plasmas of pig, bull, and dog.

Purification of HSP-3 to homogeneity was achieved by a three-step, non-denaturing chromatographic procedure. Affinity chromatography on heparin-Sepharose makes it possible to recover HSP-3 in the non-binding fraction (Fig. 1, insert,

lane a) and free it from the bulk of the major proteins of stallion seminal plasma, HSP-1 and HSP-2 [18]. HSP-1 and HSP-2 are both mixtures of glycoforms and exist as heparin-binding (Hep^+) and non-heparin-binding (Hep^-) moieties [29,30]. Both Hep^+ and Hep^- HSP-1 and HSP-2 glycoforms, however, display phosphorylcholine-binding affinity [19]. Hence, HSP-3 was separated from contaminating Hep^- HSP-1 and Hep^- HSP-2 by chromatography on phosphorylcholine-agarose (Fig. 1, insert, lane b). Finally, HSP-3 was purified by size-exclusion chromatography (Fig. 1, insert, lane c). This purification protocol yields typically ~70% of the initial amount of HSP-3, i.e. 65 ± 5 mg HSP-3/100 ml seminal plasma (0.9 mg HSP-3/ml seminal plasma).

HSP-3 elutes from the size-exclusion chromatography column as a 25 kDa protein. The protein is pure as judged by electrospray ionisation mass spectrometry (Fig. 1). HSP-3 is a non-glycosylated protein and displays a p*I* of 8–9 by two-dimensional electrophoresis. Hence, contrary to rat epididymal protein DE [12], the primogenitor and the most studied member of the CRISP family, mouse CRISP-1 [31], and SGP28, a human neutrophil specific granule protein of 28 kDa [32], all of which are acidic or neutral glycoproteins, HSP-3 is a basic glycosylated protein.

The molecular mass of HSP-3, determined by mass spectrometry, is 24 987 ± 3 Da (Fig. 1). HSP-3 is N-terminally blocked [18]. Carboxymethyl (CM) cysteine was not detected by amino acid analysis of hydrolysates of non-reduced HSP-3 which had been previously denatured with guanidine hydrochloride and treated with iodoacetamide. However, 15.6 ± 2 CM-cysteine residues were found in hydrolysates of reduced, iodoacetamide-treated HSP-3. These data indicate that, like other CRISP molecules, native HSP-3 may contain eight disulphide bonds [15,31] and that mature HSP-3 corresponds to residues ^{23}QDPGF...ENKIY^{223} of its cDNA-deduced amino acid sequence (EMBL entry AJ001400) (M_r calculated: 24 993, assuming pyroglutamic acid as N-terminal residue, and all cysteine residues engaged in disulphide bonds).

Analytical ultracentrifugation showed that HSP-3 displays a molecular mass of 26.4 ± 0.2 kDa and a sedimentation coefficient of 2.4 ± 0.1 S, showing that HSP-3 is made of a single polypeptide chain displaying monomer behaviour in solution.

3.2. Topography and quantitation of HSP-3 on spermatozoa

Indirect immunofluorescence microscopy was employed to assess the localisation of HSP-3 on stallion sperm. The protein was localised on the postacrosomal region of the head and on the mid-piece of fresh ejaculated sperm separated from seminal plasma by centrifugation and washed three times with PBS (Fig. 2D). On average, 0.9–9 × 10^6 HSP-3 molecules were quantitated in PBS-washed sperm from different animals, strongly suggesting that HSP-3 might bind to an abundant membrane compound, i.e. a lipid moiety.

HSP-3, like rat DE protein [13], binds to the heads of spermatozoa. This topography appears to be different from that reported for rat DE protein, which was originally localised on the dorsal region of the sperm head and shown to migrate to the equatorial segment with the occurrence of the acrosome reaction [33]. However, other recently published results [34] show an association of rat epididymal protein 4E9 (which is identical to DE protein [35]) with the tail region of spermatozoa, and a role in sperm maturation has been proposed. Moreover, contradictory results have been published on CRISP-1. Thus, Krätschmar et al. [15] have reported that CRISP-1 does not bind to human spermatozoa, whereas Fujimoto and colleagues [36] have shown that this protein binds to the postacrosomal region of the sperm head. Interestingly, antibodies against guinea pig and bovine sperm fertilin molecules, proteins that, like rat DE protein, have been proposed as sperm-egg membrane fusion candidates, stained the postacrosomal sperm head [37,38]. As a whole, the large amount

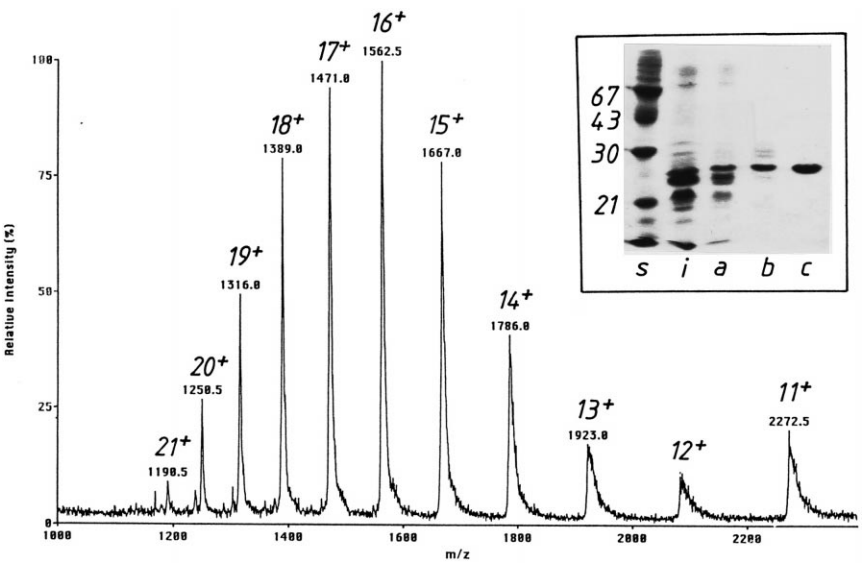

Fig. 1. Electrospray ionisation mass spectrum of isolated HSP-3. Signals covering the complete series of protonated quasimolecular ions with 11–21 positive charges are shown. Insert: Silver-stained SDS-polyacrylamide electrophoretic gel of chromatographic fractions along the purification procedure of HSP-3: lane i, complete stallion seminal plasma used as initial material for chromatography on heparin-Sepharose; lane a, non-heparin-binding proteins; lane b, non-phosphorylcholine-binding proteins; lane c, HSP-3 purified by Sephadex G-50 size-exclusion chromatography. Molecular masses (in kDa) of standard proteins separated in lane s are shown at the left, from top to bottom: bovine serum albumin, ovalbumin, carbonic anhydrase, and soybean trypsin inhibitor.

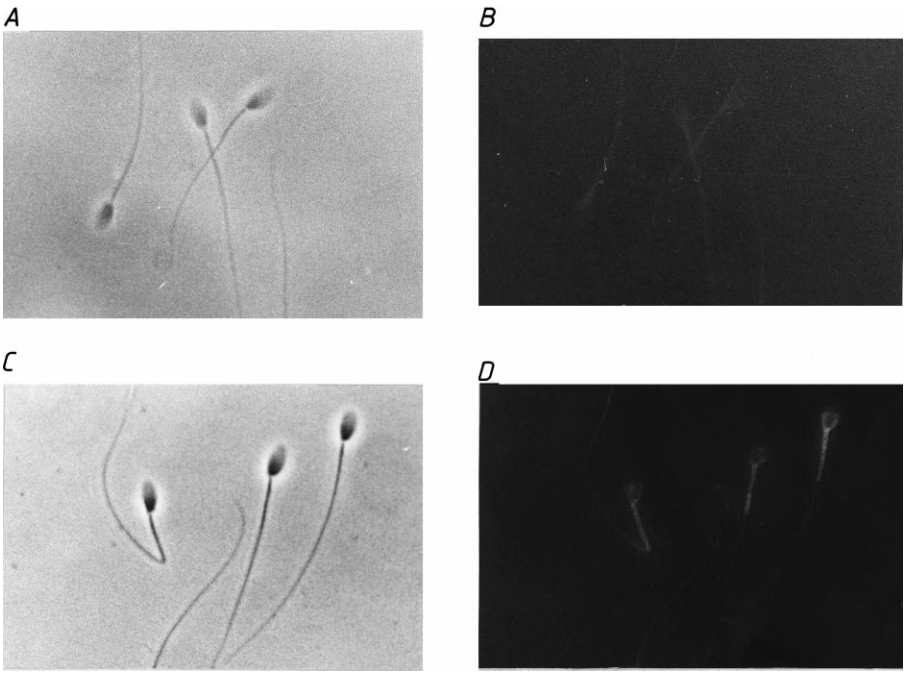

Fig. 2. Localisation of HSP-3 epitopes on PBS-washed (D) stallion spermatozoa by indirect immunofluorescence. B: Control run by omission of the primary antibody. A and C: Phase-contrast microscopy of the samples shown in B and D, respectively.

of sperm-coated HSP-3 and its topography would support a role for HSP-3 in sperm maturation and/or gamete interaction similar to that suggested for rat DE (4E9) glycoprotein.

3.3. *Secondary and tertiary structure of HSP-3 probed by CD and FTIR spectroscopies*

The far- and near-UV CD spectra of HSP-3 in 20 mM HEPES pH 7.0 at 25°C are depicted in Fig. 3A and B, respectively. The near-UV spectrum of HSP-3 consists of a major negative band with two discrete peaks at 288 and 297 nm overlapped to a broad band centred at about 273 nm, and a minor positive band at 253 nm. The negative fine structure at 288 and 297 nm has the characteristics expected for ^1L_b tryptophanyl bands overlapped by tyrosyl and cystine bands [39]. Such features indicate that at least several chromophores are in dynamically restricted and asymmetric environments, and that the protein is folded into a compact structure.

The far-UV spectrum of HSP-3 (Fig. 3A) displays a minor positive maximum at 235 nm and a major asymmetric negative band with a minimum at 205 nm and a shoulder at 220 nm. The chiroptic components obtained by the CCA are shown in Fig. 3C. Spectral features allow the assignment of components I and VI to non-amide chiral contributions [40,41], component II to random polypeptide structure, component III to α-helix, component IV to β-sheet and type C turns, and component V to β-sheet contributions [24,25]. It must be stressed, however, that components I and VI might include contributions arising from secondary structure elements since the ellipticity values are modified from those reported for model compounds [40,41]. Attribution of the chi-

Table 1
Secondary structure composition of HSP-3 derived by deconvolution analysis of the far-UV CD spectrum (A) and of the amide I′ band of the FTIR spectrum (B)

	Assignment	Percentage
A: Component		
I	chiral 230(+), 205(−)	17
II	random	29
III	α-helix	10
IV	β-sheet, type C turns	6
V	β-sheet	5
VI	chiral 224	33
B: Band (cm^{-1})		
1682	turns	6
1670	turns	6
1663	turns	8
1655	α-helix, solvent-shielded loops	17
1646	random, solvent-exposed loops	14
1638	random, solvent-exposed loops	16
1629	β-sheet	31
1617	low-frequency β-sheet	2

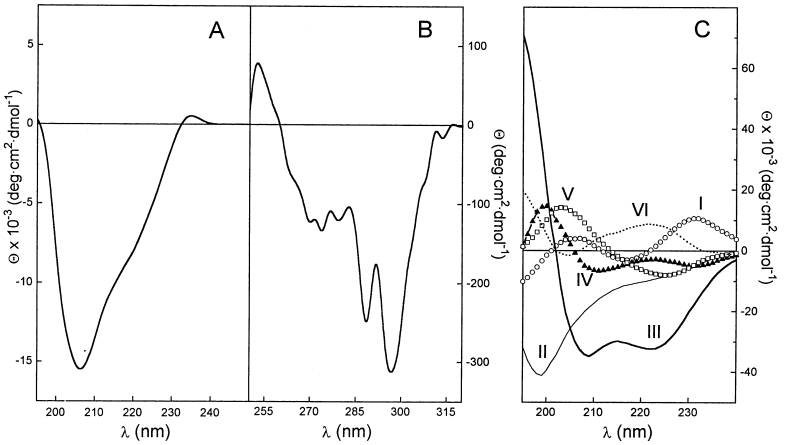

Fig. 3. Far- and near-UV CD spectra of HSP-3 at 25°C. A: Far-UV CD spectra of HSP-3 in 10 mM MOPS pH 7.0. B: Near-UV CD spectra of HSP-3 in 10 mM MOPS pH 7.0. C: CCA-derived pure chiroptic components: I and VI, non-amide chiral contributions; II, random polypeptide structure; III, α-helical conformation; IV, β-sheet and type C turns; V, β-sheet.

roptic components to secondary structure and non-amide elements is shown in Table 1.

The secondary structure of the protein was also determined from the spectral features of the FTIR spectrum in the amide I′ band. The conformational sensitive band (1700–1600 cm^{-1}) of HSP-3 displays a broad contour with a maximum at 1640 cm^{-1} (Fig. 4), which is characteristic of the stretching vibration mode of peptide carbonyl groups hydrogen-bonded to the solvent, as those located in irregular or non-ordered segments. Its resolution enhancement by Fourier-self-deconvolution reveals five bands at 1682, 1656, 1640, 1634 and 1613 cm^{-1}. Least-square iterative curve fitting into Lorentzian bands was then performed to estimate the proportion of the different secondary structure elements (Fig. 4, Table 1). Following the assignation rules developed by Goormaghtigh et al. [28], the secondary structure of HSP-3 consists of 17% of α-helix and solvent-shielded loops, 33% of β-sheets, 18% of turns and 30% of unordered segments and solvent exposed loops.

Comparison of the secondary structure percentages obtained from FTIR and CD spectroscopies reveals a good agreement in the random content, confirms the presence of helical segments, and underlines that components I and VI account not only for aromatic side chain contributions but also for turn and β-sheet arrangements. This latter observation is in fact supported by the differences in the ellipticity magnitude of the CCA-derived components as well as by the theoretical values of ellipticities estimated for a number of Trp and Tyr derivatives in a variety of environments [42]. As a whole, CD and FTIR spectroscopic analyses (Figs. 3 and 4, Table 1) both indicate that 40–50% of the primary structure of HSP-3 adopt regular secondary structure, and that HSP-3 may belong to the α+β class of proteins.

3.4. Thermal-induced transitions

Calorimetric analysis of HSP-3 in 20 mM HEPES pH 7.0 at 0.33 K/min scanning rate showed that the thermogram is characterised by a single peak centred at 64°C followed by a composition of endothermic and exothermic peaks above 80°C, revealing postdenaturation events like precipitation. The absence of endothermic signal upon reheating the solution after the first run reveals the irreversibility of the thermal denaturation. The effect of scanning rate on the thermogram was then studied to inspect a possible kinetic control in the denaturation process. The T_m value is initially shifted towards lower values as the heating rate decreases and then becomes constant at the lowest scanning rate tested (0.5 and 0.33 K/min). This type of dynamic effect is consistent with the existence of a slow relaxation process between native and reversible unfolded forms and excludes a kinetic control by the irreversible steps. Deconvolution of the curve reveals a non-two state transition characterised by a T_m of 64°C, an enthalpy change of 75 kcal/mol, and a van 't Hoff enthalpy of 184 kcal/mol. A $\Delta H_{vH}/\Delta H$ higher than 1 indicates that either the cooperative domain experimenting the transition does not exhibit all native tertiary structure contacts or that intermolecular interactions between the native or the denatured states are taking place. HSP-3 solution exhibited increase in turbidity upon heating treatment along with a downward shift in the T_m value upon increasing the protein concentration. This, together with the fact that native HSP-3 is a monomeric protein (see above), strongly indicate that deviation of the $\Delta H_{vH}/\Delta H$ ratio from the theoretical value of 1 arises from the self-associating properties of the denatured form and, subsequently, that the cooperative unfolding unit is the monomer.

Thermal denaturation of HSP-3 was also investigated by

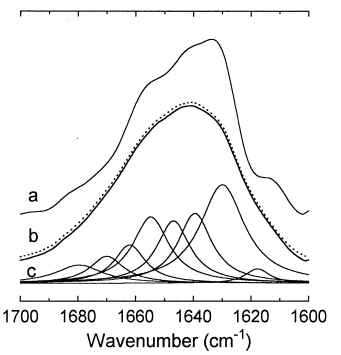

Fig. 4. Amide I′ band deconvolution into Lorentzian components of HSP-3. Self-deconvoluted amide I′ band (a), original band (b, thick line), resulting from curve fitting (b, dotted line), Lorentzian bands (c). Fourier self-deconvoluted band was scaled for graphical purposes. The result of the fit is summarised in Table 1.

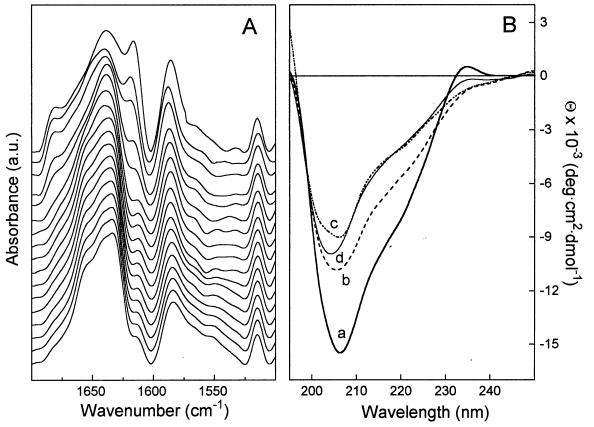

Fig. 5. Temperature dependence of the far-UV CD and FTIR spectra of HSP-3. A: Temperature-induced changes in the Fourier self-deconvoluted FTIR spectrum of HSP-3 in the 1700–1500 cm^{-1} region. Displayed spectra correspond to the following temperatures (from bottom to top): 13.5, 16, 19, 23, 28, 31.5, 34, 38, 42, 45, 50, 53, 57, 62, 66, 73, 78 and cooled to 20°C. B: Temperature-induced changes in far-UV CD spectrum of HSP-3: 25 (solid thick line, a), 75 (dashed line, b), 80 (dotted line, c) and at 25°C after cooling from 85°C (solid thin line, d).

monitoring of the temperature dependence of the Fourier self-deconvoluted IR spectrum of HSP-3 in the 1700–1500 cm^{-1} (Fig. 5). In agreement with DSC measurements, the thermal-induced unfolding of HSP-3 is irreversible as judged by non-recovery of the initial shape after cooling from the highest temperature. The deconvoluted amide I′ band contour (1700–1600 cm^{-1}) of HSP-3 remains virtually constant up to 57°C. Further heating to 61°C results in a shift of the maximum from 1634 to 1641 cm^{-1}, concomitantly with a decrease in the amide II band/amide I′ band area ratio. Above this temperature, a doublet made of a major band at 1619 cm^{-1} and a minor at 1683 cm^{-1} begins to emerge, which is characteristic of intermolecular extended structures present in the denatured states of several protein [23]. The temperature-induced variation of the far-UV CD spectrum is depicted in Fig. 5B. The spectrum remains mainly unchanged up to 61°C. Above this temperature, the definition of the maximum at 235 nm disappears, and the ellipticity undergoes a change in sign. Concomitantly, the negative band experiments a significant intensity reduction up to 80°C where it stabilises. Refolding of HSP-3 upon cooling the sample to low temperature (25°C) failed to generate the initial spectral features, thus confirming the irreversibility of the thermal-induced denaturation (see above).

Analysis of the relative changes of θ_{234}, I_{1634} and I_{1656}, assuming a two-state model, reveal a van 't Hoff enthalpy of 70.5 kcal/mol, which is similar to the calorimetric enthalpy obtained in DSC experiments and agrees with a native-to-unfolded monomer form one-step transition. On the contrary, when similar analysis is performed for the relative changes of θ_{205}, I_{1619} and I_{1683} the obtained values account for 170 ± 10 kcal/mol which resembles the van 't Hoff enthalpy derived from the calorimetric analysis, suggesting that these parameters are related to the appearance of irreversible aggregated unfolded forms. It deserves special mention the fact that $T_{1/2}$ values derived from CD spectroscopical analysis are upward shifted in the temperature scale compared with the values derived from FTIR measurements. This apparent discrepancy has its origin in the protein concentrations used for the different spectroscopical measurements and agrees with the downward shift in T_m observed by DSC upon decreasing the protein concentration.

3.5. Possible structure-function correlations

Analysis of CRISP molecule sequences has allowed the identification of two regions. The N-terminal 170 amino acid region (mouse CRISP-1 numbering) contains three disulphide bonds between Cys^{60}–Cys^{137}, Cys^{76}–Cys^{151}, and Cys^{132}–Cys^{148} [34]. The C-terminal domain 171–224 forms a compact structure crosslinked by five disulphide bonds and resistant to enzymatic degradation [31]. Calorimetric and spectroscopical analysis of HSP-3 thermal denaturation fails in the identifications of these two regions as independent cooperative domains. Although structural data are not available for CRISP molecules, the single irreversible calorimetric unfolding transition exhibited by HSP-3 suggests that the majority of the secondary structure elements may be located in the N-terminal domain. This domain displays significant amino acid sequence similarity with proteins originating from phylogenetically distant organisms like insects (hornet venom allergen antigen 5.1), plants (pathogenesis-related protein-1 or PRP-1), and fungi (fruiting body proteins sC7 and sC14) (for a multiple sequence alignment, see Fig. 7 in [17]). These insect, plant, and fungi proteins lack the C-terminal cysteine-rich region supporting the hypothesis of distinct physiological roles for the N- and C-terminal CRISP domains. On the other hand, PRP-1, sC7 and sC14 are expressed upon infection and exhibit fungicidal activity, suggesting a role for these proteins in host defence. Similarly, due to its subcellular location in specific granules, a potential anti-microbial action of neutrophil CRISP SGP 28 has been suggested [32]. The expression of mouse CRISP-3 in B lymphocytes has led to the hypothesis that CRISP-3 is also a defence-associated molecule in mammals [43]. Murphy and co-workers [44] have report the cloning of a cDNA encoding GliPR, a protein of the CRISP family that is highly expressed in the human brain tumour glioblastoma multiform/astrocytoma, but neither in normal foetal or adult brain tissue, nor in other nervous system tumours. GliPR shares up to 50% amino acid sequence similarity with plant PRP-1, and the authors speculate that there may be functional similarities between the human and the plant proteins. Moreover, helothermine is a peptide toxin of the CRISP family isolated from the venom of the Mexican beaded lizard [17], which block ryanodine receptor channels in a cell-free system. Thus, a hypothetical role for HSP-3 (and other CRISPs) as an anti-infectious agent in seminal plasma deserves further detailed studies.

The crystal structure of the antifungal protein zeamatin [45], and $\alpha+\beta$ protein member of the pathogenesis-related protein family 5 distantly related to PRP-1, reveals an electrostatically polarised surface, suggesting that it exerts fungicidal activity by destabilisation of hyphal membranes through electrostatic interactions. Similar mechanism has been proposed for a variety of structurally unrelated cell-lytic, antifungal and antibacterial peptides [46–48]. Thus, it is tempting to speculate that the putative host defence and/or membrane fusion activities of CRISPs (i.e. free in secretion and sperm surface-associated, respectively) could result from perturbation of the barrier function of the target membrane. The large amounts of CRISP HSP-3 that can be isolated from stallion seminal plas-

ma and the biochemical and conformational characterisation of this protein reported here may pave the way for further biophysical studies aiming to investigate its biological role.

Acknowledgements: This work has been financed by Grants Ca209/1-1 from the Deutsche Forschungsgemeinschaft, Bonn, Germany, PB95-0077 and PB96-0850 from the Dirección General de Investigación Científica y Técnica, Madrid, Spain, and BMBF 01KY9503 from the Bundesministerium für Bildung, Forschung und Technologie, Bonn, Germany. A.M.S. is a recipient of Fellowship GRK 158/2-96 (Graduiertenkolleg 'Zell- und Molekularbiologie in der Tiermedizin') from the Deutsche Forschungsgemeinschaft, Bonn, Germany.

References

[1] Yanagimachi, R. in: The Physiology of Reproduction (Knobil, E. and Neill, J.D., Eds), 2nd edn., pp. 189–317, Raven Press, New York.
[2] Bedford, J.M., Moore, H.D.M. and Franklin, L.E. (1979) Exp. Cell Res. 119, 119–126.
[3] Talbot, P. and Chacon, R.S. (1982) Fertil. Steril. 248, 354–360.
[4] Clark, J.M. and Köhler, J.K. (1990) Mol. Reprod. 27, 351–365.
[5] Myles, D.G. (1993) Dev. Biol. 158, 35–45.
[6] Wolfsberg, T.G. and White, J.M. (1996) Dev. Biol. 180, 389–401.
[7] Snell, W.J. and White, J.M. (1996) Cell 85, 629–637.
[8] Rochwerger, L., Cohen, D. and Cuaniscú, P.S. (1992) Dev. Biol. 153, 83–90.
[9] Allen, C.A. and Green, D.P.L. (1995) J. Cell Sci. 108, 767–777.
[10] Cuaniscú, P.S., Conesa, D. and Rochwerger, L. (1990) in: Gamete Interaction. Prospects for Immunocontraception (Alexander, N.J., Griffin, D., Spieler, J.M. and Waites, G.M.H., Eds.), pp. 143–153, Wiley-Liss, New York.
[11] Cuaniscú, P.S. and Rochwerger, L. (1991) in: Comparative Spermatology: 20 Years After (Bachetti, B., Ed.), pp. 555–560, Raven Press, New York.
[12] Brooks, D.E., Means, A.R., Wright, E.J., Singh, S.P. and Tiver, K.K. (1986) Eur. J. Biochem. 161, 13–18.
[13] Rochberger, L. and Cuaniscú, P.S. (1992) Mol. Reprod. Dev. 31, 34–41.
[14] Cohen, D.J., Munuce, M.J. and Cuaniscú, P.S. (1996) Biol. Reprod. 55, 200–206.
[15] Krätzschmar, J., Haendler, B., Eberspaecher, U., Roosterman, D., Donner, P. and Schleuning, W.-D. (1996) Eur. J. Biochem. 236, 827–836.
[16] Foster, J.A. and Gerton, G.L. (1996) Mol. Reprod. Dev. 44, 221–229.
[17] Morrissette, J., Krätzschmar, J., Haendler, B., El-Hayek, R., Mochca-Morales, J., Martin, B.M., Patel, J.R., Moss, R.L., Schleuning, W.-D., Coronado, R. and Possani, L.D. (1995) Biophys. J. 68, 2280–2288.
[18] Calvete, J.J., Nessau, S., Mann, K., Sanz, L., Sieme, H., Klug, E. and Töpfer-Petersen, E. (1994) Reprod. Dom. Anim. 29, 411–426.
[19] Calvete, J.J., Raida, M., Gentzel, M., Urbanke, C., Sanz, L. and Töpfer-Petersen, E. (1997) FEBS Lett. 407, 201–206.
[20] O'Farrell, P.H. (1975) J. Biol. Chem. 250, 4007–4021.
[21] Heukeshoven, J. and Dernick, R. (1988) Electrophoresis 9, 28–32.
[22] Dostàlovà, Z., Calvete, J.J., Sanz, L. and Töpfer-Petersen, E. (1994) Biochim. Biophys. Acta 1200, 48–54.
[23] Menéndez, M., Gasset, M., Laynez, J., Lopez-Zumel, C., Usobiaga, P., Töpfer-Petersen, E. and Calvete, J.J. (1995) Eur. J. Biochem. 234, 887–896.
[24] Perczel, A., Park, K. and Fasman, G.D. (1992) Anal. Biochem. 203, 83–93.
[25] Perczel, A., Hollósi, M., Tusnády, G. and Fasman, G.D. (1991) Protein Eng. 4, 669–679.
[26] Vuilleumier, S., Sancho, J., Loewenthal, R. and Fersht, A.R. (1993) Biochemistry 32, 10303–10313.
[27] Romero, A., Pineda-Lucena, A. and Giménez-Gallego, G. (1996) Eur. J. Biochem. 241, 453–461.
[28] Goormaghtigh, E., Cabiaux, V. and Ruysschaert, J.M. (1990) Eur. J. Biochem. 193, 409–420.
[29] Calvete, J.J., Reinert, M., Sanz, L. and Töpfer-Petersen, E. (1995) J. Chromatogr. A 711, 167–173.
[30] Calvete, J.J., Mann, K., Schäfer, W., Sanz, L., Reinert, M., Nessau, S., Raida, M. and Töpfer-Petersen, E. (1995) Biochem. J. 310, 615–622.
[31] Eberspaecher, U., Roosterman, D., Krätzschmar, J., Haendler, B., Habernicht, U.-F., Becker, A., Quensel, C., Petri, T., Schleuning, W.-D. and Donner, P. (1995) Mol. Reprod. Dev. 42, 157–172.
[32] Kjeldsen, L., Cowland, J.B., Johnson, A.H. and Borregaard, N. (1996) FEBS Lett. 380, 246–250.
[33] Cameo, M.S., González-Echeverría, M.F., Blaquier, J.A. and Burgos, M.H. (1986) Gamete Res. 15, 247–258.
[34] Moore, A., Ensrud, K.M., White, T.W., Frethem, C.D. and Hamilton, D.W. (1994) Mol. Reprod. Dev. 37, 181–194.
[35] Xu, W., Ensrud, K.M. and Hamilton, D.W. (1997) Mol. Reprod. Dev. 46, 377–382.
[36] Hayashi, M., Fujimoto, M., Takano, H., Ushiki, T., Abe, K., Ishikura, H., Yoshida, M.C., Kirchhoff, C., Ishibashi, T. and Kasahara, M. (1996) Genomics 32, 367–374.
[37] Primakoff, P., Hyatt, H. and Tredick-Kline, J. (1987) J. Cell Biol. 104, 141–149.
[38] Waters, S.I. and White, J.M. (1997) Biol. Reprod. 56, 1245–1254.
[39] Strickland, E.H. (1974) Crit. Rev. Biochem. 2, 113–175.
[40] Auer, H.E. (1973) J. Am. Chem. Soc. 95, 3003–3011.
[41] Hooker, T.M. and Schellman, J.A. (1970) Biopolymers 9, 1319–1348.
[42] Woody, R.W. (1995) Methods Enzymol. 246, 34–71.
[43] Pfisterer, P., König, H., Hess, J., Lipowsky, G., Haendler, B., Schleuning, W.-D. and Wirth, T. (1996) Mol. Cell Biol. 16, 6160–6168.
[44] Murphy, E.V., Zhang, Y., Zhu, W. and Biggs, J. (1995) Gene 159, 131–135.
[45] Batalia, M.A., Monzingo, A.F., Ernst, S., Roberts, W. and Robertus, J.D. (1996) Nature Struct. Biol. 3, 19–23.
[46] Saberwal, G. and Nagaraj, R. (1994) Biochim. Biophys. Acta 1197, 109–131.
[47] Fahrner, R.L., Dieckmann, T., Harwig, S.S.L., Lehrer, R.I., Eisenberg, D. and Feigon, J. (1996) Chem. Biol. 3, 543–550.
[48] Lacadena, J., Martínez del Pozo, A., Gasset, M., Patiño, B., Campos-Oliva, R., Vázquez, C., Martínez-Ruiz, A., Mancheño, M. and Gavilanes, J.G. (1995) Arch. Biochem. Biophys. 324, 273–281.